Available online at www.sciencedirect.com
SCIENCE DIRECT®

Journal of the European Ceramic Society 23 (2003) 1655–1660

www.elsevier.com/locate/jeurceramsoc

Al_2O_3–Y-TZP/Al_2O_3 functionally graded composites of tubular shape from nano-sols using double-step electrophoretic deposition

Cengiz Kaya*

Interdisciplinary Research Centre (IRC) in Materials Processing and School of Metallurgy and Materials, The University of Birmingham, Edgbaston, Birmingham B15 2TT, UK

Received 12 March 2002; accepted 5 October 2002

Abstract

Al_2O_3–Y-TZP/Al_2O_3 functionally graded composites of tubular shape incorporating a very tough central layer with graded composition (Al_2O_3–Y-TZP) and a hard outer surface layer of pure alumina were produced from nano-size sols using electrophoretic deposition (EPD) in an attempt to generate a continuously inhomogeneous property variation across the final component and to control the microstructure at a nanometer scale. It is shown that hardness, fracture toughness and alumina grain size within the graded layer are controlled by the volume fraction of TZP grains and the highest volume fraction (71%) of TZP phase provides a fracture toughness value of 7.1 MPa $m^{1/2}$ and Vicker's hardness of 10.4 GPa whilst the lowest volume fraction (13%) results in obtaining a fracture toughness value of 3.8 MPa $m^{1/2}$ and hardness value of 15.7 GPa. The pure alumina surface layer (100 μm in thickness) with a high hardness value of 19.4 GPa is considered to be beneficial for tribological applications where high wear resistance is required.
© 2003 Elsevier Science Ltd. All rights reserved.

Keywords: Al_2O_3–ZrO_2; Electrophoretic deposition; Functionally graded materials; Hardness; Toughness

1. Introduction

The need for new materials with tailored properties and different functions at different surfaces has led to exploration of the phase gradation that has been long established in nature. These graded structures, seen in such examples of culms of bamboo and barley, on bone and seashell, have been the main driving force for extensive work to produce similar microstructures from metal/ceramic, metal/metal or ceramic/ceramic compositions.[1–6] The concept behind this significant research effort is that the chemical composition and/or microstructure across the component can be controlled in order to control the property gradation. The resultant composites are referred to as functionally graded materials (FGMs) and they possess unique properties for a variety of applications such as fuel cells, biomaterial implants, thermal barriers, and materials for energy conversion. A variety of processing techniques including powder processing, electrochemical processing and filtration, field activated synthesis, thermal or plasma spraying, microwave processing and chemical vapour deposition have been proposed to manufacture such graded components.[7–11] However, these methods are generally complicated, time consuming and also expensive for large scale production in industry; therefore electrophoretic deposition (EPD) has been introduced as an alternative to produce gradient materials.[12,13] EPD is accepted as a novel, relatively simple, cost-effective and high forming-rate technique for producing monolithic/multilayer ceramics and fiber-reinforced composites.[14–20] This process relies on the presence of charged particles in liquid suspension, i.e. a sol, which, on the application of an electric field, will move and be deposited on an oppositely charged electrode. The rate of deposition is high and can be controlled by controlling the applied potential.

In the present work, tubular Al_2O_3–Y-TZP/Al_2O_3 functionally graded composites incorporating a tough

* Tel.: +44-121-414-3537; fax: +44-121-414-3441.
E-mail address: c.kaya@bham.ac.uk (C. Kaya).

0955-2219/03/$ - see front matter © 2003 Elsevier Science Ltd. All rights reserved.
PII: S0955-2219(02)00370-9

central layer with graded composition (Al_2O_3–Y-TZP) and a hard outer surface layer of pure alumina were produced from nano-size sols using EPD in an attempt to generate a continuous property variation across the final component and to improve the microstructural features in terms of grain size, hardness and fracture toughness.

2. Experimental work

Two different colloidal sols, i.e. pure alumina and alumina plus Y–TZP, to be used in the EPD experiments were prepared. In order to obtain the Al_2O_3–Y-TZP structure after sintering, equal amounts of very fine (the average particle size is 30 nm, VP zirconia, Degussa Ltd, Germany), medium size (150 nm, BDH Chemicals, UK) and coarse (400 nm, Dai-chi Ltd, Japan) zirconia powders were first dispersed in distilled water with the addition of 3 mol% Y_2O_3. To prepare a kinetically stable zirconia sol, the distilled water was stirred vigorously while the nano-size zirconia powders were added at a rate of 0.5 g min^{-1}. The low rate of addition prevented the formation of large heteroflocculated clusters. The resultant sol and 0.5 wt.% binder (Celacol, in order to increase the green strength) were then added to a boehmite sol (γ-AlOOH) containing spherical particles with an average particle size of 100 nm (Alcan Chemicals, UK) and then ball-mixed all together for 1 day (the boehmite sol was seeded with 2 wt.% TiO_2 particles in order to lower the α-alumina transformation temperature). The solids-loading of the final sol was adjusted to be 20 wt.% of the dispersion liquid with simultaneous ultrasonic agitation to enhance powder dispersion. Homogeneous, well-dispersed and agglomerate-free stable suspensions were obtained at a pH value of 9.2.

A commercial α-Al_2O_3 powder (Tai-micron, Japan) was used as the pure alumina source. As received alumina powders contain spherical particles with an average particle size of 150 nm. These powders were dispersed in distilled water at a pH value of 4 with the addition of 0.5 wt.% binder (Celacol) and the solids-loading of the prepared suspension was adjusted to be 20 wt.% of the dispersion medium. The final sol was ball-mixed for 1 day.

An in-situ electrophoretic deposition cell was used in order to manufacture functionally graded components.[17] A stainless steel rod 0.3 mm in diameter was used as deposition electrode (+) whilst a tubular stainless steel electrode 40 mm in diameter was used as the negative electrode (cathode). The central electrode was coated with a very thin C layer in order to allow easy removel of the EPD formed green deposit before sintering. The distance between the two electrodes was chosen to be 17 mm. The EPD cell electrodes were connected to a 0–60 V d.c. power supply. The first stage of EPD was performed with the Al_2O_3–Y-TZP sol under a constant voltage of 10 V using a deposition time of 2.5 min and with magnetic stirring during the EPD. Under the applied electric field, the boehmite and zirconia particles (possessing a net negative surface charge at pH 9.2) migrated towards the positive electrode, i.e., the deposition electrode (see Fig. 1). The particles were deposited until a matrix thickness of 1.4 mm was achieved. The central deposition electrode was connected to a balance linked to a computer. The apparatus

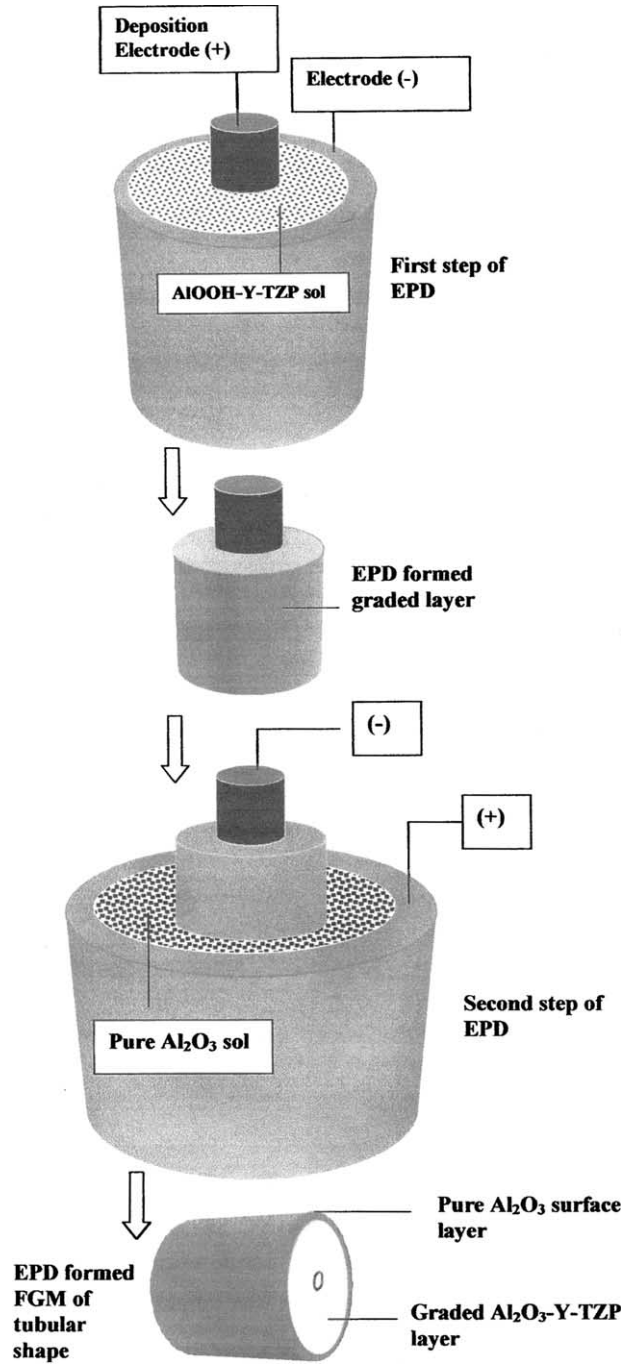

Fig. 1. Processing of Al_2O_3–Y-TZP/Al_2O_3 FGM of tubular shape using double-step EPD.

is able to record the weight gain per millisecond during the deposition process, i.e., in real time. After the first stage EPD, the deposition electrode surrounded with the boehmite plus zirconia deposit layer in green state was put in the pure alumina suspension and the central deposition electrode was connected to the negative terminal of the power supply as alumina particles have positive surface charge at the working pH value of 4. The second stage EPD was performed using the same voltage of 10 V d.c. for a deposition time of 1.5 min in order to obtain a thin alumina layer around the first formed thicker boehmite plus zirconia layer. The final green body specimens in tubular shape containing an inner layer of boehmite plus zirconia surrounded by a thin layer of pure alumina were dried under humidity controlled atmosphere for 1 day and left in ambient air for another day before being pressureless sintered at 1400 °C for 2 h.

The surface properties of the colloidal sol particles in terms of their electrophoretic mobility and net surface charge were determined using a surface charge analyser (DELSA 440 surface charge analyser). Microstructural observations were carried out by using a field emission gun scanning electron microscope (FEG SEM, Hitachi FX-4000, Japan) on sintered, fractured and thermally etched (1300 °C for 20 min) surfaces. Fracture toughness and hardness were determined using the Vickers indentation technique.[21] Grain size measurements were conducted using the linear intercept technique.[22] and the interfacial behaviour of the composites between the graded layer and the pure alumina surface layer was characterised using the crack path propagation technique.[23]

3. Results and discussion

The sintered (1400 °C for 2 h) microstructure of the tubular Al_2O_3–Y-TZP/Al_2O_3 functionally graded composite incorporating a tough central layer with graded composition (Al_2O_3–Y-TZP) and a hard outer surface layer of pure alumina is shown in Fig. 2. From the SEM picture it is clear that the thickness of the outer alumina layer is about 100 μm indicating the ability of electrophoretic deposition to produce a homogeneous and controlled surface layer. It is also seen from Fig. 2 that the pure alumina surface layer is continuous and homogeneous in thickness and also that there is no crack formation within the graded layer or alumina surface layer. The FGM produced has a central hole 0.25 mm in diameter, a layer of Al_2O_3–Y-TZP 1.4 mm in diameter and a surface alumina layer 100 μm in thickness. In order to analyse the composition within the graded section of the composite, detail SEM pictures were taken from the points shown in Fig. 2 and the amount of alumina and Y–TZP phases were calculated

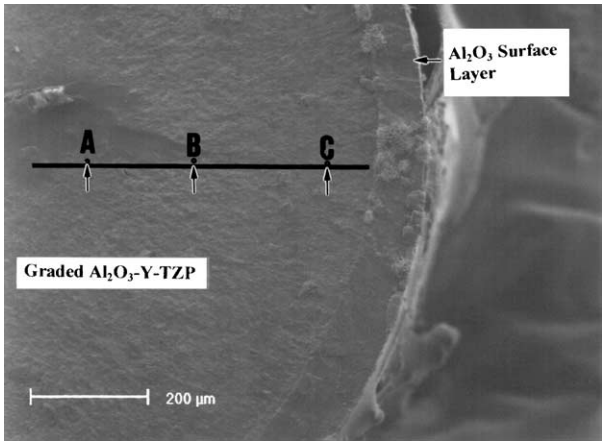

Fig. 2. SEM micrograph of the EPD-formed FGM of tubular shape showing the XRD and SEM analysed points within the graded layer and the thickness of the pure alumina surface layer to be 100 μm.

using X-ray diffraction and also an image analyser for comparison.

The graded internal layer of Al_2O_3–Y-TZP is formed by the controlled and engineered EPD using nano sol particles having different particle sizes. The electrophoretic mobility of each particle within the mixed sol will be different as this depands on the particle sizes, and hence the masses.[14,17] Particles with smaller diameter will have higher mobility than those of larger size. The SEM pictures shown in Fig. 3 indicate the difference in composition from the centre to the alumina layer proving the validity of the 'particle mobility-particle size relationships' concept. The SEM micrograph shown in Fig. 3a represents the microstructure at the point A (dark phase is alumina and the light phase is TZP). The volume fraction of the TZP phase was found to be 71% at this point ($r = 150$ μm). The composition of the graded layer shows a gradual change in composition as shown in Fig. 3b and c. The volume fraction of TZP phase decreases from 35% (point B, $r = 350$ μm) to 13% (point C, $r = 550$ μm). SEM pictures taken along the radius of the sintered FGM show an increase in alumina volume fraction from the centre to the pure alumina layer and they also show a significant change in microstructure as shown in Fig. 3. Table 1 shows the relationships between the composition of the graded layer and the grain size of the alumina and TZP grains. The finest alumina grain size (0.65 μm) was found at the point A where the volume fraction of TZP is 71% whilst this value increases to 1.85 μm at the point C when the TZP volume fraction decreases to 13%. However, the TZP grain size along the radius of the FGM seems to be independent of the composition. The SEM microstructure of the pure alumina surface layer is shown in Fig. 3d indicating the presence of a dense microstructure with an average alumina grain size of 2.6 μm. It can be concluded from the results presented in Fig. 3 that the TZP grains

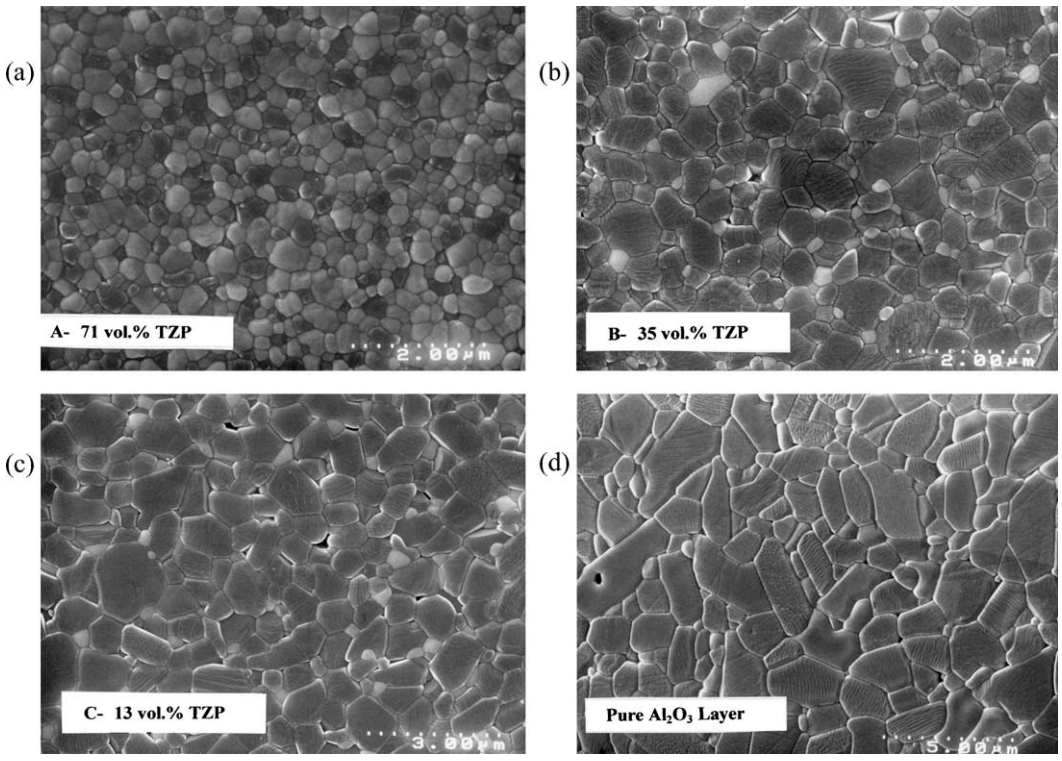

Fig. 3. SEM micrographs taken from the points within the Al_2O_3–Y-TZP graded layer shown in Fig. 2: (a) 71 vol.% TZP (point A), (b) 35 vol.% TZP (point B), (c) 13 vol.% TZP (point C) and (d) the microstructure of pure alumina surface layer (dark phase represents alumina and the light phase represents TZP grains.

Table 1
Properties of electrophoretically formed Al_2O_3–Y-TZP/Al_2O_3 FGM of tubular shape

Area in graded layer (see Fig. 2)	Grain size (μm)		Volume fraction of TZP (%)	Hardness (GPa)	Fracture toughness (MPa $m^{1/2}$)
	Al_2O_3	TZP			
A	0.65	0.70	71	10.4	7.1
B	1.35	0.75	35	12.9	6.3
C	1.85	0.85	13	15.7	3.8
Pure Al_2O_3 layer	2.6	–	0	19.4	3.1

within the graded layer play an important role in suppressing alumina grain growth, the highest volume fraction providing sub-micron alumina grains within the graded layer.

The relationships between the composition of the FGM and hardness/fracture toughness are also given in Table 1. As the volume fraction of TZP phase within the functionally graded Al_2O_3–Y-TZP layer decreases, the hardness value increases whilst the fracture toughness decreases. The highest toughness value of 7.1 MPa $m^{1/2}$ was determined at the point A and the highest hardness value of 15.7 GPa at the point C. It is also seen from the Table 1 that the pure alumina surface layer has a hardness value of 19.4 GPa and a moderate fracture toughness value of 3.1 MPa $m^{1/2}$, resulting from the dense and fine grained alumina microstructure.

The SEM micrographs of fracture surfaces of the graded layer and pure alumina surface layer are shown in Fig. 4a and b, respectively. Inter-granular fracture is the dominant failure mode for both layers, however, a few alumina grains within the pure alumina surface layer fail trans-granularly, as shown in Fig. 4b. The presence of fine, medium size and also coarser TZP grains within the graded layer is visible from the image shown in Fig. 4a. The nature of the interfacial region between the graded Al_2O_3–Y-TZP and the pure Al_2O_3 surface layer in terms of the crack deflection and propagation behaviour was characterised by using a crack path propagation test, as shown in Fig. 4c. An indenter-induced crack propagates intergranularly from the pure alumina surface layer and when it interacts with the graded layer, it propagates along the

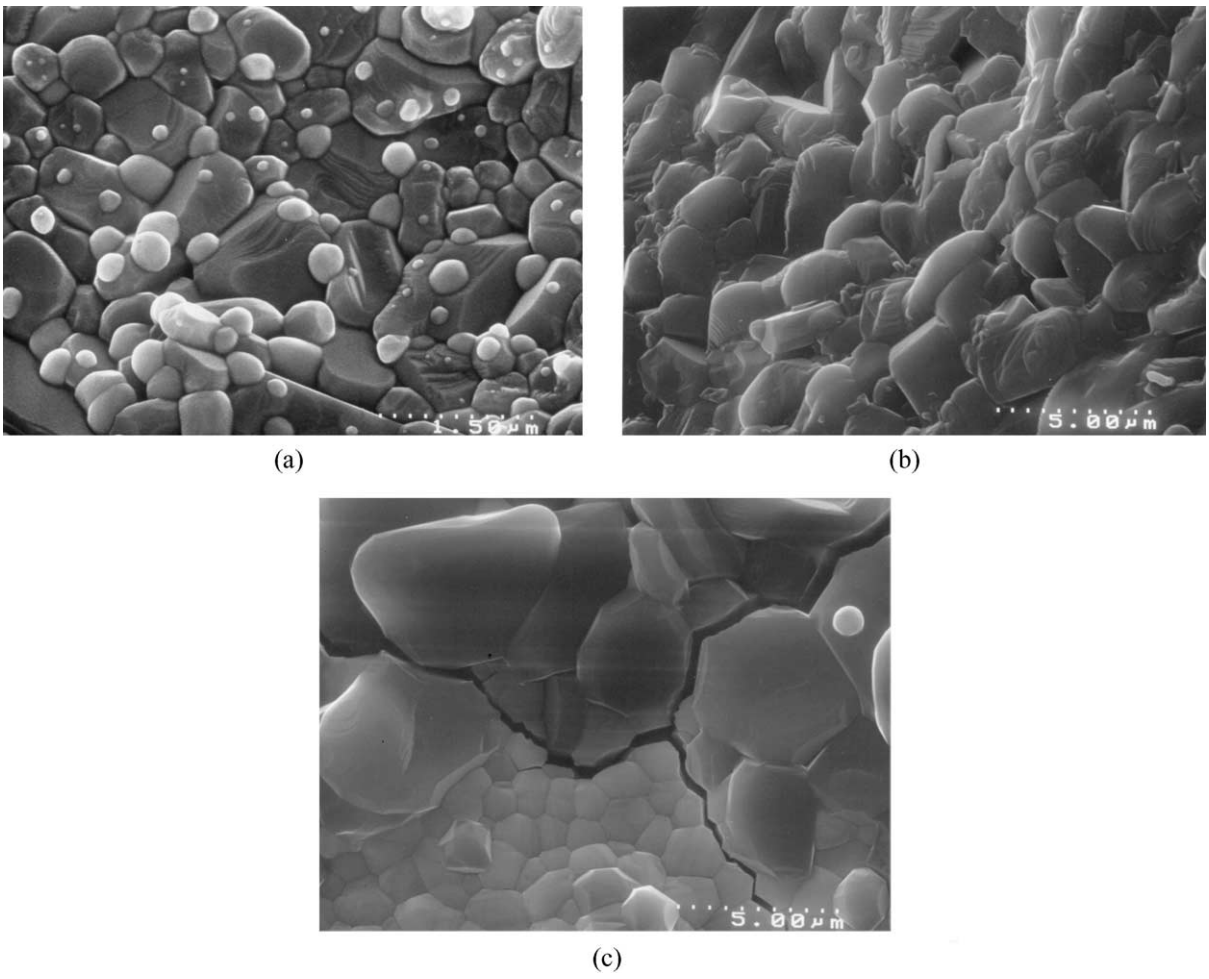

Fig. 4. SEM micrographs of the fracture surfaces of (a) Al_2O_3–Y-TZP graded layer, (b) pure alumina surface layer, both showing dominantly intergranular fracture behaviour and (c) intergranular propagation of an indenter-induced crack along the graded and surface alumina grain boundary.

graded layer and pure alumina boundary. Fig. 4c shows that the bonding between these two phases is weak enough to deflect a crack which should contribute to the damage-tolerant behaviour of the overall FGM composites.

4. Conclusions

Electrophoretic deposition (EPD) was used to produce tubular Al_2O_3–Y-TZP/Al_2O_3 functionally graded composites incorporating a tough central layer with graded composition (Al_2O_3–Y-TZP) and a hard outer surface layer of pure alumina from nano-size sols in an attempt to generate a continuous property variation across the final component and to control the microstructure at a nanometer scale. Hardness, fracture toughness and alumina grain size within the graded layer were found to be controlled by the volume fraction of TZP grains and the highest volume fraction (71%) of TZP phase provides a fracture toughness value of 7.1 MPa $m^{1/2}$ and Vicker's hardness of 10.4 GPa whilst the lowest volume fraction (13%) results in a fracture toughness of 3.8 MPa $m^{1/2}$ and hardness of 15.7 GPa. Increase in volume fraction of TZP phase within the graded layer decreases hardness and increases the fracture toughness and also controls the alumina grain growth during sintering. Pure alumina surface layer (100 μm in thickness) with a hardness value of 19.4 GPa is introduced for tribological applications. The FGM composite shows mainly intergranular fracture behaviour and the interfacial region between the graded layer and the alumina surface layer is weak as an indenter-induced crack propagates intergranularly along the boundary between these two phases. The results presented in this work suggest that the overall FGM produced could be an ideal micro-component for room and high temperature applications where "damage-tolerant" behaviour and high wear resistance are required. Experimental work is being conducted at present in order to determine the thermomechanical properties of the FGM.

Acknowledgements

Profs. P. Bowen and S. Blackburn are acknowledged for the provision of laboratory facilities in the School of Metallurgy and Materials and the IRC in materials processing, respectively. Partial financial support by the European Commission under the contract number BRITE-EURAM, BRPR-CT 97-0609 is also acknowledged.

References

1. Lin, C. Y., McShane, H. B. and Rawlings, R. D., Extrusion process for manufacture of bulk functionally graded materials. *Powder Metall*., 1996, **39**, 219–222.
2. Rawlings, R. D., Tailoring properties—functionally graded materials. *Mater. World*, 1995, **3**, 474–475.
3. Zhang, W. F., Xi, N. S., Tao, C. H., Han, J. C. and Du, S. Y., Microstructure and resisting thermal shock behaviours of TiC–Al_2O_3/Fe functionally graded materials prepared by SHS/PHIP. *J. Mater. Sci. Technol*., 2001, **17**, 65–66.
4. Zhao, C., Vandeperre, L., Basu, B. and Van Der Biest, O., Cylindirical Al_2O_3/TZP functionally graded materials by EPD. *Brit. Ceram. Trans*., 2000, **99**, 284–287.
5. Oike, S. and Watanabe, Y., Development of in-situ Al–Al_2Cu functionally graded materials by a centrufugal method. *Int. J. Mater. Prod. Tec*., 2001, **16**, 40–49.
6. Ishibashi, H., Tobimatsu, H., Matsumoto, T., Hayashi, K., Tomsia, A. P. and Saiz, E., Characterization of Mo–SiO2 functionally graded materials. *Metall. Mater. Trans*., 2000, **31A**, 299–306.
7. Daniel, M. P., Levin, L. and Frage, N., Graded ceramic preforms: various processing approaches. *Materials Chemistry and Physics*, 2001, **67**, 192–198.
8. Miyamoto, Y., Kaysser, W. A., Rabin, B. H., Kawasaki, A. and Ford, R. G., *Functionally Graded Materials: Design, Processing and Applications*. , 1999.
9. Jedamzik, R., Neubrand, A. and Rödel, J., Functionally graded materials by electrochemical processing and infiltration: application to tungsten/copper composites. *J. Mater. Sci*., 2000, **35**, 477–486.
10. Koizumi, M., FGM activities in Japan. *Compos. Part B. Eng*., 1997, **28**, 1–4.
11. Mortensen, A. and Suresh, S., Functionally graded metals and metal-ceramic composites: part 1, processing. *Int. Mater. Rew*., 1995, **40**, 239–265.
12. Kirihara, S., Tomota, Y. and Tsijimoto, T., Application of an intermetallic compound Ti5Si3 to functionally graded materials. *Mat. Sci. Eng. A*, 1997, **240**, 600–604.
13. Sarkar, P., Datta, S. and Nicholson, P. S., Fuctionally graded ceramic/ceramic and metal/ceramic composites by electrophoretic deposition. *Comp. Part B—Eng*., 1997, **28**, 49–56.
14. Moritz, K., Thauer, R. and Muller, E., Electrophoretic deposition of nano-scaled zirconia powders prepared by laser evaporation. *CFI*, 2000, **77**, E8.
15. Kaya, C. Processing and Properties of Alumina Fibre-reinforced Mullite Ceramic Matrix Composites. *PhD Thesis*, The University of Birmingham, UK, June 1999.
16. Harbach, F. and Nienburg, H., Homogeneous functional ceramic composnents through electrophoretic deposition from stable colloidal suspensions—II. Beta-alumina and concepts for industrial production. *J. Eur. Ceram. Soc*., 1998, **18**, 685–692.
17. Kaya, C., Boccaccini, A. R. and Chawla, K. K., Electrophoretic deposition forming of nickel-coated-carbon-fibre-reinforced borosilicate-glass-matrix composites. *J. Am. Ceram. Soc*., 2000, **83**, 1885–1888.
18. Kaya, C., Kaya, F., Boccaccini, A. R. and Chawla, K. K., Fabrication and characterisation of Ni-coated carbon fibre-reinforced alumina ceramic matrix composites using electrophoretic deposition. *Acta Mater*., 2001, **49**, 1189–1197.
19. Negishi, H., Sakai, N., Yamaji, K., Horita, T. and Yokokawa, H., Application of electrophoretic deposition technique to solid oxide fuel cells. *J. Electrochemical Soc*., 2000, **147**, 1682–1687.
20. Kaya, C., Butler, E. G., Boccaccini, A. R. and Lewis, M. H., Processing and characterisation of mullite (Nextel™ 720) fibre-reinforced mullite matrix composites from hydrothermally processed mullite precursors. In *High Temperature Ceramic Matrix Composites (HT-CMC 4)*, ed. W. Krenkel, R. Naslain and H. Schneider. WILEY-VCH, Weinheim, Germany, 2001, pp. 639–644.
21. Anstis, G. R., Chantikul, P., Lawn, B. R. and Marshall, D. B., A critical evaluation of indentation technique for measuring fracture toughness. I—direct crack measurement. *J. Am. Ceram. Soc*., 1982, **64**, 533–538.
22. Mendelson, I. M., Average grain size in polycrystalline ceramics. *J. Am. Ceram. Soc*., 1969, **52**, 443–446.
23. Morgan, P. E. D. and Marshall, D. B., Ceramic composites of monozite and alumina. *J. Am. Ceram. Soc*., 1995, **78**, 1553–1563.